

# Simulation of Missiles with Grid Fins using an Actuator Disc

Ph. Reynier \* and J. M. Longo \*

DLR, Lilienthalplatz 7, 38108 Braunschweig, Germany

E. Schülein \*

DLR, Bunsenstraße 10, 37073 Göttingen, Germany

An actuator disc for grid fin simulations has been integrated in the DLR's TAU unstructured code. With this method the physical grid fins are replaced by artificial boundary conditions in the flow for the numerical simulations. The objective in using an actuator disc is to reduce the computational effort during the design loops of vehicles equipped with grid fins. The forces produced by the grid fins are computed using a procedure based on the semi-empirical theory for lattice wings and coupled with the code. The final tool is applied to the predictions of force and moment coefficients around a missile with grid fins. The numerical predictions are compared with the experimental data obtained at DLR for a Mach number range from 1.8 to 4 and different angles of attack. In addition, computations for a body alone have been performed to be used as a reference to assess the code capabilities in recovering the experimental differences of force and moment coefficients between the complete missile and the body alone. The results for several Mach numbers show the capability of the method to predict the differences found experimentally between the drag of the vehicle and the body. The numerical simulations with angle of attack show good agreement with the experiments for force coefficients and pitching moment. This work shows the capabilities of the tool at different Mach numbers and angles of attack and its usefulness for the design of vehicles equipped with grid fins.

## Nomenclature

- $c$ : plane thickness of the grid fin  
 $c_f$ : skin friction coefficient  
 $c_x$ : axial force coefficient  
 $c_{x_f}$ : axial friction coefficient  
 $c_{x_i}$ : axial lift coefficient  
 $c_{x_p}$ : integrated surface pressure force coefficient  
 $c_{x_w}$ : axial wave drag coefficient  
 $h$ : grid fin height  
 $n$ : number of cells in a grid fin  
 $s$ : thickness of the grid fin internal frame  
 $t$ : thickness of the grid fin external frame  
 $t_{yz}$ : size of a square lattice wing cell  
 $t_y$ : horizontal size of a lattice wing cell  
 $t_z$ : vertical size of a lattice wing cell  
 $x, y, z$ : cartesian coordinates  
 $y^+$ : dimensionless value of  $y$   
 $C_d$ : drag coefficient  
 $C_m$ : pitching moment  
 $C_x$ : axial force coefficient  
 $C_z$ : normal force coefficient  
 $Ma$ : Mach number  
 $Ma_{cr1}$ : first critical Mach number  
 $Ma_{cr2}$ : second critical Mach number  
 $Ma_{cr3}$ : third critical Mach number  
 $S_x$ : surface area of the grid fin perpendicular to the  $x$  direction  
 $S_y$ : surface area of the grid fin perpendicular to the  $y$  direction  
 $S_z$ : surface area of the grid fin perpendicular to the  $z$  direction

## Introduction

**S**INCE the middle of the eighties, the lattice wings also called grid fins or lattice controls have been the object of a strong interest in the scientific community working on missile technology. In 1998, several papers presented at the *Applied Vehicle Technology Panel Symposium* held in Sorrento (Italy) were focused on this topic.<sup>1–4</sup> Other studies

on lattice wings have been carried out in Canada, Russia, Taiwan and the United States. Some were dedicated to experimental investigations,<sup>5–7</sup> others to theoretical analysis<sup>8,9</sup> or to numerical computations of missiles with lattice wings<sup>10–12</sup>). Some investigations were dedicated on the experimental investigation of an isolated lattice wing<sup>13</sup> and the numerical simulation of the flow inside a grid fin cell.<sup>14</sup>

The aerodynamic qualities of grid fins have been known for a long time and have already been listed<sup>4</sup>. They are very effective control devices and sometimes have advantages over planar fins.<sup>4</sup> Their performance in the supersonic regime and their relatively small size make them very attractive for missile applications. They present two main disadvantages, they suffer a loss of stability in the transonic regime and have relatively high drag levels. The first disadvantage<sup>3</sup> is due to the fact that the grid fin cells choke in the transonic regime. The high drag levels of grid fins has been the main concern which has for many years restricted the use of this technique. However, recently some experimental studies<sup>15</sup> have shown that grid fin drag levels can be considerably reduced by altering the frame cross-section shape and the web thickness with only a minimal impact on lift and other aerodynamic properties.

Several numerical studies<sup>10–12</sup> have been dedicated to flow simulation of vehicle equipped with grid fins. Generally, the results show that Navier-Stokes computations of missiles with grid fins compare well with experimental data. The same investigations have highlighted that the predictions obtained with an Euler approach were not appropriate for these flows. However, the Navier-Stokes simulations are expensive due to the complexity of the geometry which requires 80 % of the mesh to be located in the grid fin region.<sup>10</sup>

Since the nineties, different research activities on grid fins have been conducted in Germany. This topic has focused the interest of DLR<sup>16</sup> but also of industry<sup>17</sup> for high supersonic missiles. In the past years, several test campaigns have been led<sup>18</sup> to investigate different geometries of lattice wings and missiles with grid fins in order to create a large experimental database devoted to these controls. In parallel to these experiments, numerical investigations have been undertaken. In order to save some computational effort, a methodology based on the actuator disc technique has been developed<sup>19,20</sup> to simulate flows around a vehicle with lattice wings. Using this approach, the lattice wings are replaced by an actuator disc and therefore, by artificial boundary conditions inside the flow, where the forces produced by the grid fins are taken into account in the balance

\*Research engineer, Institut für Aerodynamik und Strömungstechnik

Received 29 January 2004; revision received 2 February 2005 accepted for publication 3 February 2005. Copyright © 1997 by the American Institute of Aeronautics and Astronautics, Inc. No copyright is asserted in the United States under Title 17, U.S. Code. The U.S. Government has a royalty-free license to exercise all rights under the copyright claimed herein for Governmental Purposes. All other rights are reserved by the copyright owner.

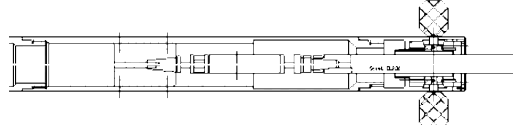


**Fig. 1** Missile with lattice wings experimentally investigated by Esch.<sup>18</sup> In the picture, the wings are parallel to the body for visualisation purposes.

equations. Initially, this method<sup>19,20</sup> was coupled to an experimental database providing the force coefficients at the lattice wing locations. Several simulations have been performed for an isolated grid fin<sup>19</sup> and a complete vehicle<sup>20</sup> experimentally investigated by Esch.<sup>18</sup> The comparisons with the experimental data<sup>20</sup> have demonstrated the capabilities of the method but also the strong dependence of the numerical result reliability on the database range of validity.

The actuator disc for lattice wings is now integrated in the TAU<sup>21</sup> unstructured solver developed by DLR. This allows some new savings of mesh generation effort. In the current study, the actuator disc has not been coupled with an experimental database but with a numerical procedure based on the semi-empirical theory for lattice wings.<sup>8</sup> Using this procedure, the forces at the lattice wing location are computed as functions of geometrical parameters and flow conditions using semi-empirical formulae. The numerical tool has already been successfully applied to the prediction of the force coefficients of an isolated grid fin.<sup>23</sup> In the current effort, the code is applied to the prediction of the aerodynamic performance, in terms of force and moment coefficients, of a complete vehicle. This will assess the capacity of the tool to be used for the design of high supersonic vehicles equipped with grid fins.

## Numerical aspects

### Flow solver

The code TAU,<sup>21</sup> developed by DLR, has been used for the numerical simulations. It solves the three-dimensional Navier-Stokes equations, written in a conservative form, using a finite volume approach and can handle structured, unstructured and hybrid meshes built with prisms, pyramids, tetrahedra and hexaedra. Different numerical schemes are available for the flux discretisation using upwind (AUSM, Roe, Van Leer,...) or central discretisation (scalar or matrix dissipation). Dissipation terms are also added to damp high frequency oscillations. For the current study, the AUSM-DV scheme has been retained. The final scheme is accurate to the second order in space. The integration in time is carried out through an explicit Runge-Kutta scheme. For accelerating the convergence, techniques like local time stepping, residual smoothing and multigrid are available. They have been used for the current computations. Transition modelling as well as different turbulence models are incorporated in the code, among other Baldwin-Lomax, Spalart-Allmaras and  $k - w$  model can be cited. Unsteady flows can also be handled by the code and special features like grid deformation and Large Eddy Simulation can be used. Additional numerical techniques like chimera and low Mach number preconditioning are also incorporated in the code. A module for grid adaptation is also available and has been used to check the grid dependence of the results. This tool is vectorised and parallelised.

### Actuator disc

An actuator disc is an artificial discontinuity inside a flow. This theory has been extensively described by Horlock.<sup>25</sup> According to this author, this concept dates back to the

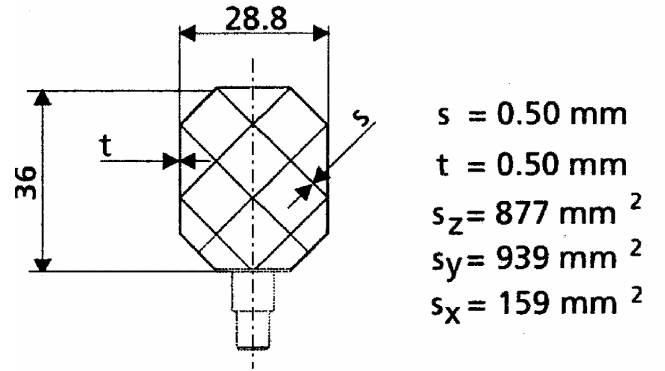


**Fig. 2** Grid fin with its support, experimentally investigated by Esch<sup>16,18</sup> and numerically studied here.

Rankine-Froude theory of the flow through a ship propeller. Since then, the actuator disc concept has been used to model a wide range of engineering problems such as helicopter rotors, windmills or multistage turbo-machines. Here, this technique is applied to model lattice wing effects for predicting the flow around a missile with grid fins. In order to reduce the computational cost of the simulations around this geometry, an actuator disc has been initially developed.<sup>19,24</sup> The geometrical details of the missile and the grid fins are represented in Figures 1 and 2. Using an actuator disc, each lattice wings is replaced by a set of artificial boundary conditions inside the flow.<sup>19,20</sup>

The actuator disc theory is based on the application of the conservation laws for mass, momentum and energy. Using this technique, the grid fin is replaced by two sets of boundary conditions. At the upstream side of the actuator disc, the characteristic theory is applied. Therefore, all the variables are extrapolated for a supersonic flow, while one has to be imposed for a subsonic flow. Here, for a subsonic flow the density and velocity components are extrapolated from inside the domain and the mass-flux is chosen as the variable to be prescribed. Its value at the downstream boundary of the actuator disc is imposed while pressure and energy are calculated supposing that the total enthalpy remains constant.

The characteristic theory is also used at the downstream side of the actuator disc. As a consequence, four flow properties have to be imposed if the flow is subsonic while the fifth is extrapolated from inside the flow-field. The velocity has been chosen as the variable to be extrapolated. For a supersonic flow, all the variables have to be imposed. In this case, all the flow variables at the downstream boundary are calculated from their respective values at the upstream boundary of the actuator disc. The local aerodynamic forces produced by the presence of the grid fin are accounted for in the flux balance at the downstream side of the actuator disc. These forces are computed with a semi-empirical module, described hereafter, as functions of the local flow conditions and geometrical parameters.

These boundary conditions, developed for laminar flows, have been extended to turbulent flows using Neumann boundary conditions for the turbulent quantities at the actuator disc. Of course, this is a very rough approximation which does not account for the impact of the lattice wing on the turbulence. The clarification of this point, which would be an important target for a future study has not been examined here.

### Semi-empirical module

Downstream of the actuator disc, the flow characteristics are changed due to the impact of the lattice wing. Depending on grid fin geometry and local flow conditions in terms

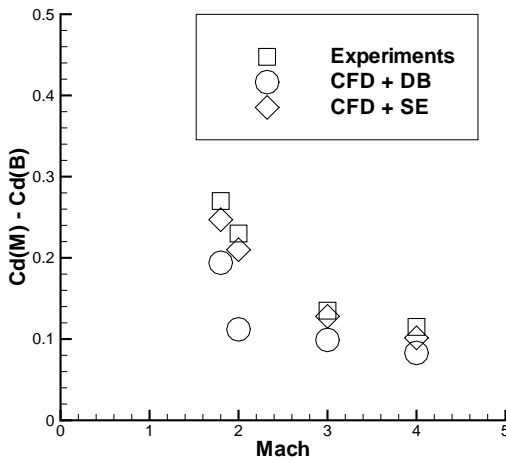


**Fig. 3** Differences between the drags of the complete missile and the body obtained experimentally (Experiments) and numerically with a database (CFD + DB)<sup>19</sup> and with the semi-empirical module (CFD + SE) in the current work.

of Mach number and pitch and yaw angles, this impact has to be determined. For the previous studies<sup>19,20</sup> carried out with the actuator disc for lattice wings, the force coefficients were interpolated from a database. This allowed an estimate of the resulting forces and moments induced by the lattice wing. The database was obtained from wind-tunnel experiments<sup>18</sup> obtained for the isolated grid fin of Figure 2 which is identical as those used for the complete missile of Figure 1. This database covered a supersonic range of Mach numbers from 1.8 to 4.

The results reported in Figure 3 show that even with a database valid for the current grid fin, the approach was not capable of recovering more than 75 % of the drag for the total vehicle for all computed Mach numbers. This was due to slight velocity deviations around the grid fin induced by the presence of the body. The grid fin/body interactions create local conditions in term of Mach number, angle of attack and yaw angle. As a consequence the local interpolated force coefficients of the fin were not perfectly suited for the computed cases.

This situation was, of course, much worse in presence of an angle of attack, particularly in the range of Mach numbers where non linear effects are strong. The numerical predictions for a complete missile in presence of high angle of attack<sup>19,20</sup> showed some strong discrepancies with the experiments.<sup>18</sup> These discrepancies can be observed in Figure 4 where the differences between the normal forces of the complete vehicle and the body alone are plotted for the numerical simulations and the experiments. The discrepancies were strong for angles of attack higher than 10 degrees. These differences were induced by the presence of a vortical flow developing along the missile and impacting on one lattice wing. This is highlighted in Figure 5 showing the vortical flow along the missile at 10 degrees angle of attack. This points out the source of the discrepancies: the database used was not valid in presence of vortical flow due to the fact that the resulting local flow conditions were transonic while the database was only covering a Mach number range from 1.8 to 4. This previous investigation demonstrated the strong dependence of the reliability of the numerical results on the database.

Here, in order to extend the applicability of the method, the actuator disc is coupled with a numerical module<sup>22</sup> mainly based on a semi-empirical theory for lattice wings. Using this theory<sup>8</sup> which is the result of extensive experimental and numerical investigations, the force coefficients of the grid fins are computed using semi-empirical relations.

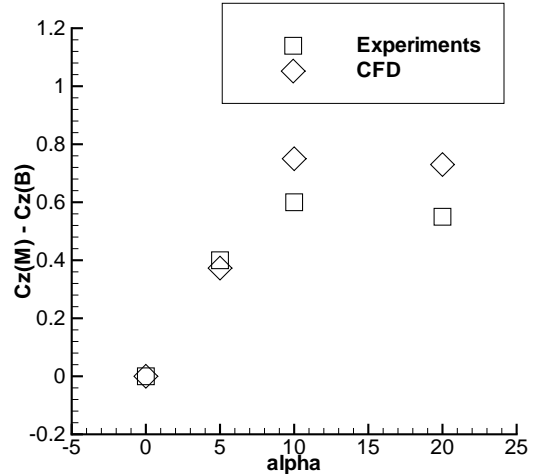


**Fig. 4** Differences between the normal forces of the complete vehicle and the body alone at Mach 1.8, in the experiments<sup>18</sup> and the numerical simulations.<sup>24</sup>

The experimental results obtained at DLR<sup>16,18</sup> for basic lattice wing configurations and a wide range of Mach numbers and angles of attack, have been used to complete and modify this theory which can be briefly described as follows. With regard to the current effort, the semi-empirical method allows the development of a predictive capability for high supersonic flight which could not be addressed using the existing experimental database.

The calculation of the grid fin performance takes advantage of the fact, that at all Mach numbers, the critical angle of attack corresponding to the maximum lift is considerably higher than for a monoplane wing. The neighbouring lifting planes of the grid fin induce a more favourable alignment of the flow. This delays the separation to higher angles of attack and causes a smooth separation at supercritical angles. The presence of orthogonal planes avoids the cross flows and gives a good basis to apply the linear theory. Each plane of a grid fin corresponds to a high aspect ratio wing. Another simplification of the theoretical model is the independence of the load capacity of a lattice wing (for given plane spacing and wing sizes) on the internal arrangement of the grid (framework or honeycomb). This hypothesis is valid for all wings with a large number of cells ( $n > 10$ ). Therefore, each cell of the wing is considered to be a square box shaped wing, and its internal flow has an aerodynamic behaviour which is completely independent. The main geometrical parameters of the lattice wing are the height  $h$ , the span  $b$ , the plane thickness  $c$  and the distances between the neighbouring vertical and horizontal surfaces  $t_y$  and  $t_z$ . Usually, the distances between the surfaces in a lattice wing are chosen in such a way that  $t_z = t_y = t_{yz}$ . These grid fin qualities simplify the calculation of the induced aerodynamic forces for the different flow regimes. A sufficiently exact prediction of the performance of these wings, at any angle of attack and yaw, is performed through a simplified formulation of the flow around the lattice wing at different speed ranges. The limits of these speed ranges can be clearly defined by characteristic flow phenomena and determined as functions of the geometrical parameters. The different speed ranges, separated by two critical Mach numbers,  $Ma_{cr1}$  and  $Ma_{cr2}$ , are the subsonic ( $Ma \leq Ma_{cr1}$ ), transonic ( $Ma_{cr1} \leq Ma \leq Ma_{cr2}$ ) and supersonic regimes (when  $Ma \geq Ma_{cr2}$ ). The supersonic regime itself is split in two by a third critical Mach number,  $Ma_{cr3}$ . Above this last critical Mach number the shock and expansion waves inside the grid fin do not impact on the neighbouring planes. The aerodynamic forces induced by lattice wings are calculated for each regime using flow conditions and geometrical

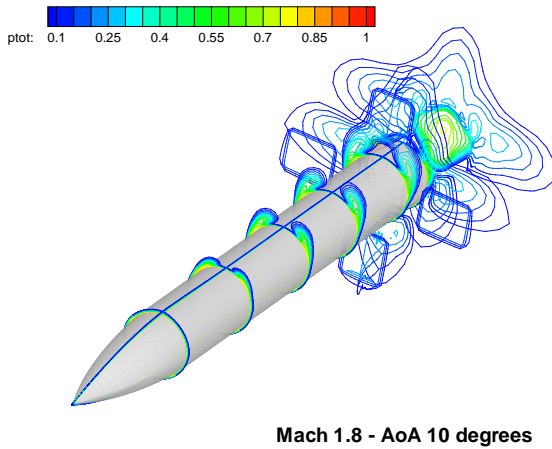


**Fig. 5** Total pressure distribution around the complete vehicle (turbulent flow, Mach 1.8, 10 degree angle of attack) simulated by Reynier & al.<sup>24</sup> with several planes in the transversal direction.

parameters.

At subsonic speeds, the calculation model is based on the lifting line scheme. The lift of the lattice wing is computed in two steps. First, each individual plane of the grid fin is supposed to be under the same conditions that one of the corresponding polyplanes with infinite span at the same effective angle of attack. Taking in consideration the lattice wing dimensions, the aerodynamic coefficients are determined using semi-empirical correlations. Then, the axial component induced by the lift has to be estimated. The lift of the grid is approximated as equal to the lift of the corresponding polyplane of infinite span. The angle of attack of the corresponding polyplane of infinite span is determined by taking into account the average downwash angle from the free vortices of the grid. Afterwards, the induced drag of the wing as well as the friction drag are calculated. An additional semi-empirical correction of the aerodynamic coefficients is determined by considering the real lattice wing dimensions.

As example, the axial coefficient of a lattice wing in a subsonic flow without flow separation is the sum of the axial friction,  $c_{x_f}$ , and lift,  $c_{x_i}$ :

$$c_x = c_{x_f} + c_{x_i}, \quad (1)$$

where the contribution of the friction is calculated from the skin friction coefficient  $c_f$ . As example for a honeycomb wing:

$$c_{x_f} = 2c_f(1 + \frac{h(b + t_{yz})}{b(h + t_{yz})}), \quad (2)$$

where  $c_f$  is computed using the usual relations valid for boundary layers. The correlations of Young<sup>26</sup> and Van Driest<sup>27</sup> are used for respectively laminar and turbulent flows. This modelling is valid until the first critical Mach number  $Ma_{cr_1}$  is reached in a grid cell.

The model for transonic flows is applied when the sonic speed is reached in the narrowest cross section of the wing. This corresponds to the critical Mach number  $Ma_{cr_1}$ . A restructure of the flow-field takes place inside the grid fin at this regime characterized by the formation of strong shock waves and local supersonic zones. This involves an increase of the axial force of the wing through an additional wave drag  $c_{x_w}$  which comes additionally to the known parts of Equation 1:

$$c_x = c_{x_f} + c_{x_i} + c_{x_w}. \quad (3)$$

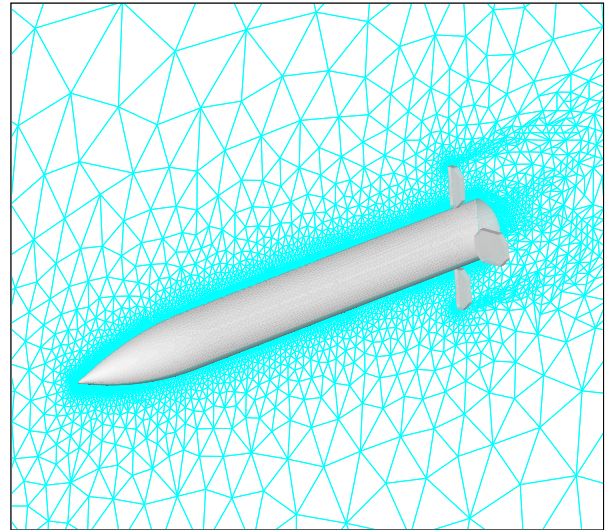


**Fig. 6** Symmetry plane of the hybrid mesh used to compute the complete vehicle.

The axial wave drag of the lattice wing,  $c_{x_w}$ , can be split in two components, one from inside the flow and the other from outside. Both parts are calculated with different simplified theoretical models adapted using empirical equations.

The following physical model is applied for the calculation of the lift coefficient. The analogy between the flow inside the grid cells and the one dimensional channel flow is used. It is well known, that after the achievement of the sound speed in the throat of a convergent-divergent channel, the conditions remain critical also at higher subsonic speeds. As a consequence, the incoming flow upstream of the channel intake is isentropically braked by the upstream influence until the critical Mach number  $Ma_{cr_1}$  is reached. This involves the reduction of the mass-flux through the channel throat. These conditions can be calculated and the effect on the lift coefficient determined by comparison with the reference value at  $Ma_{cr_1}$  using the relationship of the dynamic pressures at the channel entrance and in the undisturbed incoming flow. Finally, it is demonstrated that the variation of the normal force with the Mach number of the main flow ( $Ma_{cr_1} \leq Ma \leq 1$ ) or the subsonic flow behind the head wave ( $1 \leq Ma \leq Ma_{cr_2}$ ) is proportional to the variation of the dynamic pressure. The total drag of the wing is increased additionally by the wave drag, which can be calculated using an empirical correlation depending on the wing geometry.

With the achievement of the supersonic regime in the incoming flow at  $Ma \leq Ma_{cr_1}$ , a normal head shock wave moves upstream of the wing. There is no change in the flow inside the grid cells since the flow behind this head wave is subsonic. The wing drag changes since the strong shock wave leads to additionally total pressure losses.

The supersonic regime begins when the second critical Mach number,  $Ma_{cr_2}$ , is reached. At this regime, the head shock wave becomes attached to the leading edges of the planes. The definition of  $Ma_{cr_2}$  used in this work corresponds to a higher Mach number, at which the flow becomes supersonic in the complete flow-field between the neighbouring planes. In the region where  $Ma > Ma_{cr_2}$ , the flow between two planes of the lattice wing at moderate incidence angles can be calculated with analytic equations. Considering the emerging interactions of expansion fans or shock waves in different combinations together or with solid walls, the pressure distributions on the wing surface and the induced forces (without friction drag) can be determined. As a result of the mutual interaction between the planes, the lift coefficient of the lattice wing in this region is reduced comparing to the typical value for isolated planes. The axial

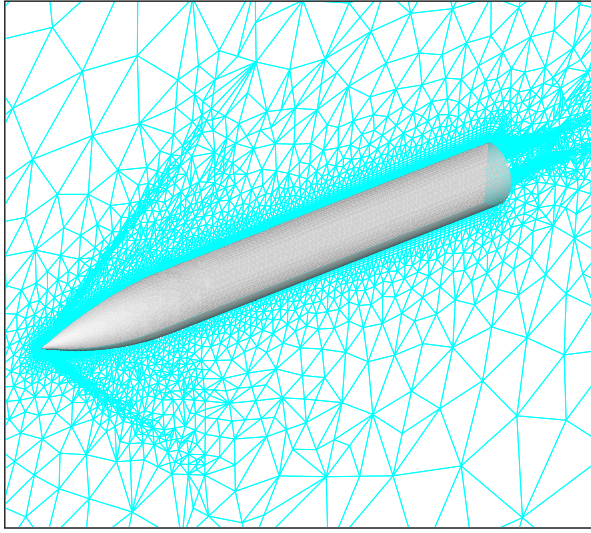


**Fig. 7** Symmetry plane of the hybrid mesh used to compute the body alone.

force coefficient can be calculated as:

$$c_x = c_{x_f} + c_{x_p}, \quad (4)$$

where  $c_{x_p}$  is provided by the integration of the surface pressure. The friction component  $c_{x_f}$  is calculated like at smaller Mach numbers. For a honeycomb wing, Equation (2) can be used.

At higher Mach numbers, another critical Mach number is reached:  $M_{cr3}$ . Above this Mach number, the shock waves and the expansion waves do not impact on the neighbouring planes. The surface pressure distribution on each wall is independent and corresponds to the one of an isolated plane. Therefore, the previous physical model remains valid and is applied for the calculation of the force coefficients. The semi-empirical module has been validated with experimental data for different grid fin design.<sup>16,18</sup> It is valid from Mach 0.3 to 6 and until 90 degree angle of attack.

#### Integration of the Actuator Disc

The actuator disc described above has been integrated in the unstructured solver TAU and the module based on the semi-empirical theory for grid fins has been coupled with the code.

Each lattice wing of the missile of Figure 1 is replaced by a set of boundary conditions. The actuator disc has exactly the same size and shape that the external frame of the grid fin. Since it was not possible to use a mesh interface with the unstructured solver, and therefore a two-dimensional actuator disc, the grid fin thickness has been retained. On the sides of the grid fin, supersonic outflow conditions are applied. Previous simulations for an isolated grid fin have shown that for subsonic flows, an inviscid wall is valid but this boundary condition produces a shock in transonic and supersonic flows. The presence of this shock induces additional drag and lift which have no reason to be, since all the contribution of the grid fin (including the external frame), in term of forces, is already taken into account by the actuator disc. This is the reason why a supersonic outflow condition is applied. The use of this boundary condition on the side of the grid fin has been already applied and validated for an isolated grid fin and a wide range of Mach numbers and angles of attack.<sup>23</sup> Only the grid fin arm (see Figure 2) is neglected for the computations.

The actuator disc consists of two surfaces with a priori two different meshes. To apply the actuator disc boundary conditions, each point of a boundary uses the values of the flow variables on the other boundary. As a consequence, for each computational point of an actuator disc side, a mirror point has been created on the other side. At the mirror point,

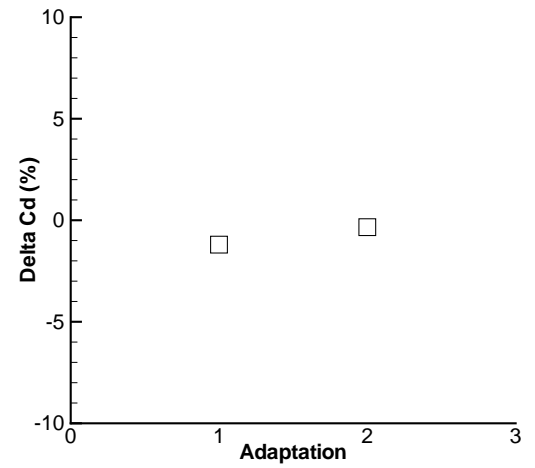


**Fig. 8** Evolution of the drag of the complete missile, in %, during the mesh adaptation process for a laminar flow at Mach 4.

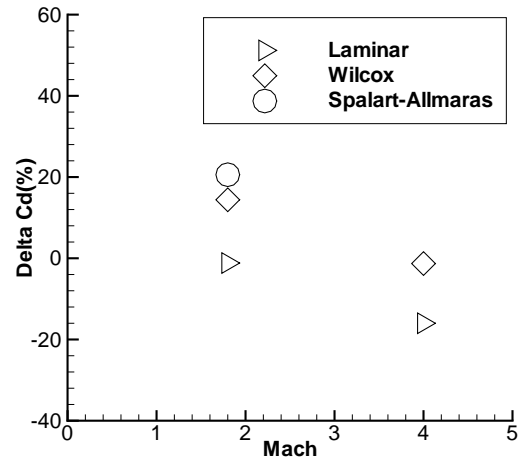


**Fig. 9** Differences in % between the experimental and numerical values of the drag for the body alone at Mach 1.8 and 4.

the values of the necessary variables are interpolated from the neighbouring points. On the upstream and downstream surfaces, the relevant actuator disc boundary conditions are applied. This is done for each point of the surfaces.

Downstream of the grid fin, the flow has been modified. Using the semi-empirical module, based on lattice wing theory, the local aerodynamic forces induced by the grid fin are calculated as functions of the local flow conditions (Mach number, angles of attack and yaw) and grid fin geometrical characteristics (height, chord, span, spacing and plane thickness). This is done for each point of the actuator disc downstream surface. In this way, all the local flow perturbations are accounted for. This is particularly efficient to take into account the local effects due to the interactions between the fins and the body.

The final code has been already applied on an isolated grid fin.<sup>23</sup> This has demonstrated the capability of the tool to reproduce, for this geometry, the trends of the force coefficient evolution for a wide range of Mach numbers (from Mach 0.8 to 4) and angles of attack (from 0 to 20 degrees). Here, the tool is applied to the simulation around a complete missile to determine the influence of the grid fins on the vehicle overall performances.

Case	Mach number	Reynolds number	Angle of attack	Approach
1	1.8	$1.8 \cdot 10^6$	0	Laminar
2	1.8	$1.8 \cdot 10^6$	0	Wilcox
3	2	$1.9 \cdot 10^6$	0	Wilcox
4	3	$2.5 \cdot 10^6$	0	Wilcox
5	4	$3.3 \cdot 10^6$	0	Laminar
6	4	$3.3 \cdot 10^6$	0	Wilcox
7	4	$3.3 \cdot 10^6$	0	Spalart-Allmaras
8	4	$3.3 \cdot 10^6$	5	Wilcox
9	4	$3.3 \cdot 10^6$	10	Wilcox
10	4	$3.3 \cdot 10^6$	20	Wilcox

**Table 1** Mach and Reynolds numbers, angles of attack and boundary layer modelling of the different computed cases for the complete vehicle and the body alone. The turbulence models are the two-equation  $k - \omega$  model of Wilcox and the one-equation model of Spalart-Allmaras.

## Application to a missile

### Computational Conditions

The missile with grid fins computed here has already been experimentally investigated at DLR Köln.<sup>18</sup> The geometry is represented in Figures 1 and 2. The same grid fin, taken isolated, had been previously retained to validate the numerical tool.<sup>23</sup> In the wind-tunnel tests, the model is maintained by a support which is not taken into account for the computations. It is worth noting that this support is fixed on the missile base but does not fit exactly the base. The length of the missile is 480 mm, its diameter 52 mm. The missile has a sharp nose, the length of the cylindrical afterbody is 350 mm, the lattice wings are located at 30 mm from the base and are maintained close to the body by four arms which are neglected in the numerical simulations. Due to the symmetry of the configuration, only half of the missile has been computed. In order to assess the influence of the lattice wings on the numerical results, a body alone has been also computed. This body corresponds to the vehicle described above without grid fins.

The geometries described above have been computed at Mach numbers 1.8, 2, 3 and 4. The different cases with the corresponding Mach and Reynolds numbers and angles of attack are shown in Table 1. Computations have been performed for laminar and turbulent flows. For the turbulence modelling, two models have been tested, the Spalart-Allmaras one equation model and the two-equation  $k - \omega$  model of Wilcox. Since the objective of this work is to develop a tool devoted to the design of high supersonic (or low hypersonic) vehicles with grid fins the computations with angle of attack have been performed at Mach 4. Three cases at 5, 10 and 20 degrees angles of attack have been computed in order to check the reliability of the tool in presence of angle of attack. The case 6 of Table 1 has been computed for the current configuration but also for the same missile with different grid fins in order to evaluate the code capabilities to be used as design tool for vehicle with grid fins.

The boundary conditions applied to the computational domain are as follows: the walls are isothermal, the plane  $y = 0$  is the symmetry plane and the other boundaries are the far-field. For the complete vehicle, at the lattice wing locations, the actuator disc conditions are applied.

### Meshes

The meshes used to simulate the missile and the body alone have been generated with the CENTAUR<sup>28</sup> grid generator. For both configurations (see Figures 6 and 7), the computational domains extend over a little more than half of the vehicle length in the transverse direction and one third of the vehicle length downstream of the base.

For each configuration, a first grid has been created, then adapted, adding new cells using the adaptation module of TAU<sup>21</sup> and a gradient based approach. This process has been carried out until the achievement of the grid conver-

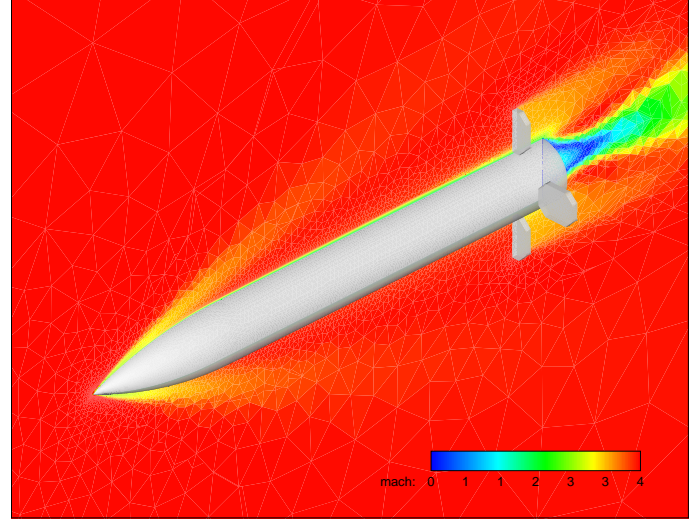


**Fig. 10** Mach number distribution around the complete missile at Mach 4 without angle of attack and with the  $k - \omega$  Wilcox turbulence model.

gence. The procedure of adaptation can be described as follows. Using a first grid, a first computation is performed, then the mesh is adapted at the shock until a constant value of the force coefficients is reached. In a second step, the mesh is converged for the complete vehicle. The last step is the optimisation of the mesh in the boundary layer, this is achieved with a  $y^+$  value lower than 1. During the mesh adaptation process, at each adaptation loop, 10 % more points were added. For the body a quite coarse mesh was initially used and around twelve adaptations were necessary to reach the grid independence of the results. For the complete vehicle the initial mesh was much finer and two to four adaptations were sufficient.

The results obtained for the successive adaptations of the mesh of the complete vehicle for a laminar flow at Mach 4 are shown in Figure 8. In this figure, the drag variation in percent is plotted. To adapt the mesh, only two adaptations were necessary, thus a total increase of 20 % of the points. At the second adaptation the drag was approximately the same as the first one with a variation lower than 0.5 %. Therefore, the mesh was considered to be converged for this case. The final meshes obtained at Mach 4 and laminar conditions, for the body alone and the complete vehicle, are shown in Figures 6 and 7. To save some effort, this meshes have been used as starting meshes for the other computations of Table 1, then, of course, the same process of mesh adaptation has been carried out. The final mesh for the complete vehicle, plotted in Figure 6, is approximately 400000 tetrahedra and 560000 prisms. For the body alone, the mesh (see Figure 7) is around 440000 tetrahedra and 490000 prisms. This demonstrates that using the actuator

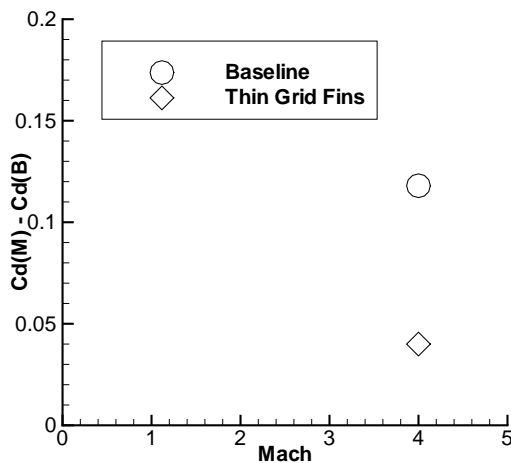


**Fig. 11 Differences between the drags of the complete missile and the body for the current lattice wings and for thinner grid fins at Mach 4.**

disc concept, the size of the mesh required for the complete vehicle is almost the same than for a body alone. When the complete vehicle is computed without the actuator disc approach, the mesh is at least five time larger than for a body alone.

#### Vehicle without angle of attack

The cases 1 to 7 of Table 1 correspond to the computations of the vehicle and the body alone at zero angle of attack. As the multigrid technique is available with TAU,<sup>21</sup> two grid levels have been used for the computations. The computations have been started using the coarse grid and finished with the fine grid in order to save some computational effort. The CFL numbers used for the simulations varied from 2 for a laminar flow without angle of attack to 0.5 for the turbulent predictions at 20 degrees angle of attack. Depending on the computed case, between 15000 and 30000 iterations were required to achieve the result convergence using the AUSM-DV numerical scheme integrated in TAU.<sup>21</sup>

At first, the influence of the turbulence modelling has been checked for a body alone. In Figure 9, the differences in % between the numerical results and the experimental data<sup>18</sup> obtained for the drag of the complete body including the base,  $C_d$ , are plotted. The simulations show a very good agreement between the laminar prediction and the experimental data at Mach 1.8. The drag is overestimated by both turbulent calculations. The Wilcox  $k - \omega$  model provides a value of the drag which is 14%, from the experimental value. This is not the case of the calculation with the model of Spalart-Allmaras where the difference with the experiments is around 20%. For this reason, this model has not been used in the other computations. At Mach 4 the experimental data is underestimated by the laminar prediction while the  $k - \omega$  model provides a good agreement. The experimental data<sup>18</sup> has been obtained for flows, which become turbulent at the shoulder of the missile. Moreover, this study is dedicated to high supersonic flows. Therefore, the approach with the  $k - \omega$  Wilcox model has been selected for all the computations of both body alone and complete missile. The discrepancies observed between the experiments and the numerical simulations are small (an order of 10%) and may originate from two sources. First, the turbulent boundary layer might not be fully developed on the body. Second, the wind-tunnel model support is not taken into account. However, this support is only fixed on a portion of the base and its contribution to the drag should be small.

The complete missile has been computed at Mach 1.8, 2, 3 and 4 with the  $k - \omega$  Wilcox model. The Mach number

distribution around the vehicle at Mach 4 is shown in Figure 10. In order to cancel the influence of the wind-tunnel model support, instead of comparing the experimental and the numerical values of the drag for the complete vehicle, the comparisons are based on the differences between the drags of the complete vehicle and the body alone obtained experimentally and numerically which are plotted in Figure 3. The results obtained in the past<sup>19</sup> are also reported in this figure. The improvement of the numerical results when using the semi-empirical module instead of an experimental database is obvious. Before, using the actuator disc technique, this was possible to recover more than 75 % of the differences between the drag of the missile and the body alone. Now, the predictions are much better. For all cases the simulations recover more than 90% of the grid fin effects. This demonstrates that the semi-empirical module is more capable to take into account local flow deviations in term of velocity and angles induced by the presence of the body and by the interactions between the grid fins and the body. However, even with the semi-empirical module the technique does not recover 100 % of the differences. In this study there is another source of discrepancy. The semi-empirical theory for lattice wings, here used, is adapted to fins with uniform cells. Due to the fact that some cells of the current grid fin differ in shape (see Figure 2), its drag is underestimated. This was also the case for the same isolated lattice wing in a previous work.<sup>23</sup> The grid cells close to the base are smaller than the others, this involves more honeycomb elements than in a uniform grid. Since the semi-empirical theory is adapted to grid fins with uniform cells, the calculations of the grid fin coefficient is performed with a model valid for a grid with less honeycomb elements. As a consequence the drag of the lattice wing of Figure 2 is underestimated. This explains why the code is not able to recover completely the lattice wing effects.

#### Design capabilities

To assess the capabilities of the code for design analysis, the complete missile has been computed with different grid fins. The vehicle is still equipped with honeycomb grid fins as in Figure 1 but the new fins have thinner inner and outer frame thicknesses. The configuration has been computed for the case 6 of Table 1. The differences between the drag of the complete missile and the body alone are reported in Figure 11. The results show that using another geometry (Thin Grid Fins) for the lattice wings, the additional drag of the complete vehicle due to the lattice wings can be considerably tailored: here, by a factor of three. The convergence of the numerical results is obtained after some hundreds of iterations and without additional mesh generation effort. This demonstrates the usefulness of the tool for system analysis during the design loops of vehicle equipped with such devices.

Furthermore, from a design point of view, an important capability of the tool is to predict the same trends as observed in the experiments. Figure 3 shows that the numerical results predict, like in the experiments, almost a drag reduction by a factor two when the Mach number increases from 1.8 to 4. This demonstrates the validity of the actuator disc to predict the force changes on a vehicle with grid fins for different Mach numbers and without angle of attack.

#### Presence of an angle of attack

In order to assess the validity of the method in presence of angle of attack, several computations have been done for 5, 10 and 20 degrees angle of attack. These calculations are reported in Table 1 as cases 8 to 10. Since the objective is to develop a numerical tool for high supersonic Mach numbers, the computations with angle of attack have been performed at Mach 4 and not at Mach 1.8 as previously.<sup>20</sup> Both complete vehicle and body alone have been computed. The predictions for the body alone are used as reference for estimating the capabilities of the actuator disc. In a

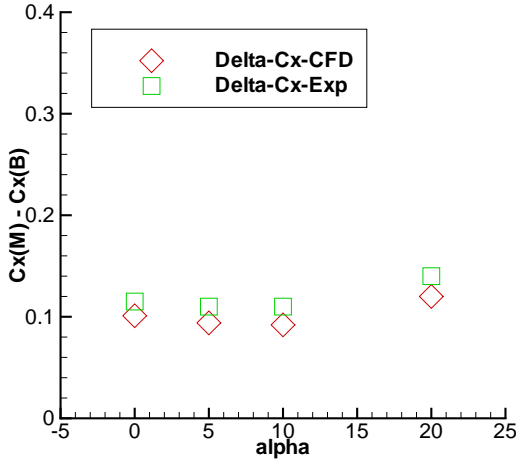


Fig. 12 Differences between the axial force coefficients of the complete missile and of the body alone as functions of angle of attack.

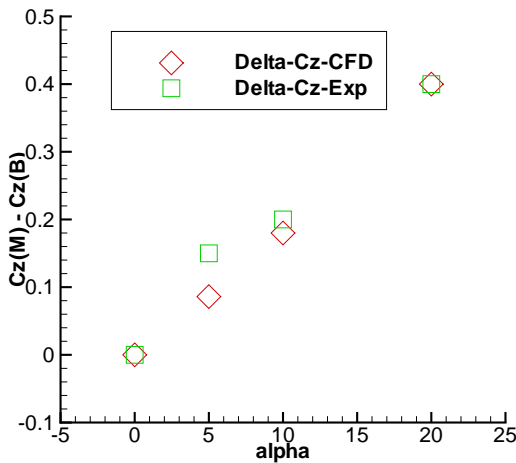


Fig. 13 Differences between the normal force coefficients of the complete missile and of the body alone as functions of angle of attack.

previous contribution,<sup>24</sup> the predictions of the axial and normal forces for both body alone and complete missile have been found to be in good agreement with the experimental data for all angles of attack. Here, the focus is on the actuator disc capabilities to recover the differences in aerodynamic coefficients between the complete missile and the body alone. For this purpose, the differences between the values predicted for the complete missile and for the body alone in the simulations and in the experiments are plotted in Figure 12 for the axial force, Figure 13 for the normal force and Figure 14 for the pitching moment. The pitching moment has been calculated taking the neutral point of the missile as reference point. Figure 12 shows a good agreement at all angles of attack between the evolution of the axial force found experimentally and numerically. More than 90 % of the differences between the axial forces of the missile and the body alone is recovered. The experimental difference is generally slightly underestimated. Like for the results without angle of attack (see Figure 3) this is due to the fact that the lattice wing used here differs in shape with the one modelled using the semi-empirical theory.

In Figure 13, the same comparison for the normal force displays good agreement except for a discrepancy at five degree angle of attack. However, the actuator disc is able to

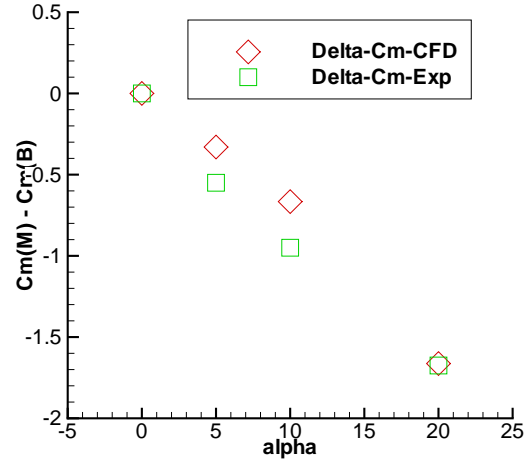


Fig. 14 Differences between the pitching moment coefficients of the complete missile and of the body alone as functions of angle of attack. The pitching moment has been calculated taking the neutral point (zero angle of attack centre of pressure) of the missile as reference point.

fairly reproduce the evolution of the forces with the angle of attack. This demonstrates the efficiency of the numerical tool in recovering the forces for the complete vehicle in presence of angle of attack. The results for the pitching moment are shown in Figure 14. They are good with some small discrepancies at 5 and 10 degrees between the differences found experimentally and numerically. Similar to the force coefficients, the tool is able to predict correctly the trend evolution of this quantity.

## Conclusions

The objective of this work was to develop a tool for the design of high supersonic missiles with lattice wings. In this objective, an actuator disc for lattice wings already tested with a structured code has been integrated in the unstructured code TAU. Instead of being coupled to an experimental database, the code has been coupled with a numerical module based on the semi-empirical theory for lattice wings providing the force coefficients as function of flow conditions and grid fin geometry. The complete tool has been applied to a missile with lattice wings. Several computations have been performed for a wide range of Mach numbers and angles of attack. In parallel, a body alone has been computed to be used as reference case for the complete vehicle.

The numerical results demonstrate the validity of the actuator disc approach for the design and the analysis of supersonic vehicles equipped with grid fins. The predictions obtained with the actuator disc coupled with the semi-empirical module and those computed previously with an experimental database have been compared. The comparisons for the prediction of the drag coefficient have demonstrated the improvements obtained when using the semi-empirical module. These improvements are due to the more extended range of validity of the semi-empirical module, in term of Mach number, angle of attack and yaw angle. Using the semi-empirical module, the local flow conditions are better taken into consideration by the numerical tool. This is particularly important to account for the body/grid fin interaction effects. The changes in force and moment coefficients experienced by the missile, due to the presence of the grid fins, are qualitatively and quantitatively very well reproduced compared to the experimental data.

The required computer time for a complete configuration on a workstation is less than 20 % more than the time required for a body alone. The extra time corresponds

to the additional mesh involved by the presence of the lattice wings and by the actuator disc. This is worth noting that a simulation of such a configuration without actuator disc would require computational effort between four and six times more than for a body alone. Another advantage of the actuator disc technique is that as long as the grid fin configuration (number of wings, size and position) remains constant, no additional time for the grid generation is necessary to test different lattice-wing geometries. Moreover, the new flow solutions are obtained with little additional computational effort. Compared to a complete simulation without actuator disc, this means an additional time saving of the order of weeks to analyse the impact of lattice wing geometry on missile performance.

## Acknowledgements

The present work has been performed in the framework of the DLR HaFK project. The financial support of the German Ministry of Defence and the project monitoring by Dr. H. Ciezki are gratefully acknowledged. This study has been partially presented at the International Symposium on Integrating CFD and Experiment in Aerodynamic held in Glasgow on September 8<sup>th</sup> and 9<sup>th</sup> 2003. The authors wish to thank the associate editor, Dr. P. Weinacht, for his advices and suggestions during the review process.

## References

- <sup>1</sup>Khalid M., Sun Y. and Xu H. "Computation of flows past grid fin missiles", *In RTO MP 5, Proceedings of RTO AVT Symposium on Missile Aerodynamics*, pp. 12.1-12.11, Sorrento, Italy, 11-14 May, 1998.
- <sup>2</sup>Kretzschmar R.W. and Burkhalter J.E. "Aerodynamic Prediction Methodology for Grid Fins", *In RTO MP 5, Proceedings of RTO AVT Symposium on Missile Aerodynamics*, pp. 11.1-11.11, Sorrento, Italy, 11-14 May, 1998.
- <sup>3</sup>Simpson G.M. and Sadler A.J. "Aerodynamic Prediction Methodology for Grid Fins", *In RTO MP 5, Proceedings of RTO AVT Symposium on Missile Aerodynamics*, pp. 9.1-9.11, Sorrento, Italy, 11-14 May, 1998.
- <sup>4</sup>Washington W.D. and Miller M.S. "Experimental investigations of grid fin aerodynamics: a synopsis of nine wind tunnel and three flight tests", *In RTO MP 5, Proceedings of RTO AVT Symposium on Missile Aerodynamics*, pp. 10.1-10.13, Sorrento, Italy, 11-14 May, 1998.
- <sup>5</sup>Brooks R.A. and Burkhalter J.E., "Experimental and analytical analysis of grid fin configurations", *Journal of Aircraft*, Vol. 26(9), pp. 885-887, 1989.
- <sup>6</sup>Burkhalter J.E., Hartfield R.J. and Leleux T.M., "Nonlinear Aerodynamic Analysis of Grid Fin Configurations", *Journal of Aircraft*, Vol. 32(3), pp. 547-554, 1995.
- <sup>7</sup>Washington W. D., Booth P. F. and Miller M. S. "Curvature and leading edge sweep back effects on grid fin aerodynamic characteristics", AIAA Paper, 93-3480-CP, AIAA Applied Aerodynamics Conference, Monterey, CA, Aug. 10, 1993.
- <sup>8</sup>Belotserkovsky S.M., Odnovol' L.A., Safin Yu.Z., Tylenev A.I., Prolov V.P. and Shitov V.A., "Reshetchatye krylia", Maschinstroenie, 320 p., Moscow, 1985.
- <sup>9</sup>Burkhalter J.E. and Frank H.M., "Grid fin aerodynamics for missile applications in subsonic flow", *Journal of Spacecraft and Rockets*, Vol. 33(1), pp. 38-44, 1996.
- <sup>10</sup>DeSpirito J., Edge H.L., Weinacht P., Sahu J. and Dinavahi P.G., "Computational fluid dynamics analysis of a missile with grid fins", *Journal of Spacecraft and Rockets*, Vol. 38(5), pp. 711-718, 2001.
- <sup>11</sup>Lin H., Huang J-C. and Chieng C-C., "Navier-Stokes computations for body/cruciform gridfin configuration", AIAA Paper, 2002-2722, 20<sup>th</sup> AIAA Applied Aerodynamics Conference, St. Louis, Mo, June 24-27, 2002.
- <sup>12</sup>Sun Y. and Khalid M. "A CFD investigation of grid fin missiles", AIAA Paper, 98-3571, 34<sup>th</sup> AIAA Joint Propulsion Conference, Cleveland, OH, July 13-15, 1994.
- <sup>13</sup>Fournier E. Y. "Wind tunnel investigation of grid fin and conventional planar control surfaces", AIAA Paper, 2001-0256, 39<sup>th</sup> Aerospace Sciences Meeting & Exhibit, Jan. 8-11, Reno, NV, 2001.
- <sup>14</sup>Lesage F. "Numerical investigation of the supersonic flow inside a cell", *In Proceedings of the 17<sup>th</sup> International Symposium on Ballistics, BALLISTICS'98*, Vol. 1, pp. 209-216, Midrand, South Africa, 23-25 March, 1998.
- <sup>15</sup>Washington W.D. and Miller M.S., "An experimental investigation of grid fin drag reduction techniques", AIAA Paper, 93-0035, 31<sup>st</sup> Aerospace Sciences Meeting & Exhibit, Reno, NV, Jan. 11-14, 1993.
- <sup>16</sup>Esch H., "Kraftmessungen an Gitterleitwerken im Überschall", DLR Internal Bericht, IB 39113-99C11, Köln, 1999.
- <sup>17</sup>Böhm G. "Aerodynamische Grundlagen und Eigenschaften von Gitterflügeln zur Steuerung von Lenkflugkörpern". IABG Bericht, B-WT 4719/02, Ottobrunn, 1994.
- <sup>18</sup>Esch H., "Aerodynamisches Beiwerte der Längsbewegung eines Flugkörpers mit Gitterleitwerk im Überschall", DLR Internal Bericht, IB 39113-2000C34, Köln, 2000.
- <sup>19</sup>Reynier Ph., Reisch U., Longo J. and Radespiel R., "Numerical study of hypersonic missiles with lattice wings using an actuator disk", AIAA Paper, 2002-2719, 20<sup>th</sup> AIAA Applied Aerodynamics Conference, St. Louis, Mo, June 24-27, 2002.
- <sup>20</sup>Reynier Ph., Reisch U., Longo J.-M. and Radespiel R., "Flow Predictions around a Missile with Lattice Wings using the Actuator Disc Concept", *Aerospace Science and Technology*, Vol. 8(5), pp. 377-388, July 2004.
- <sup>21</sup>Gerhold T., Friedrich O., Evans J. and Galle M., "Calculation of complex three dimensional configurations employing the DLR TAU code", AIAA Paper, 97-0167, 1997.
- <sup>22</sup>Schülein E., "Experten system zur Auslegung und Optimierung isolierter Gitterflügeln", DLR Internal Bericht, in preparation, Göttingen, 2003.
- <sup>23</sup>Reynier Ph. and Schülein E., "Incorporation of an actuator disc for lattice wings in an unstructured Navier-Stokes solver", *Notes on Numerical Fluid Mechanics and Multidisciplinary Design: New Results in Numerical and Experimental Fluid Mechanics IV*, pp. 132-139, Breitsamer C., Laschka B., Heinemann H.-J., Hilbig R. (Eds), Springer-Verlag, 2004.
- <sup>24</sup>Reynier Ph., Schülein E. and Longo J., "Simulation of Missiles with Grid Fins using an Unstructured Navier-Stokes solver coupled to a Semi-Empirical Actuator Disc", *In Proceedings of Conference on Integrating CFD and Experiments*, Glasgow, 8-9 Sept., 2003.
- <sup>25</sup>Horlock J. H., "Actuator disk Theory", McGraw-Hill, New-York, 1978.
- <sup>26</sup>Young, A.D., "High speed flow", *Modern Developments in Fluid Mechanics*, Ed. L. Howard, Vol. 1, pp. 375-475, Clarendon Press, Oxford, 1953.
- <sup>27</sup>van Driest, E.R., "On Turbulent Flow Near a Wall", *Journal of Aeronautical Science*, Vol.23(11), pp. 1007-1011 and 1036, 1956.
- <sup>28</sup>Anon., "Online Users Manual", <http://www.centaursoft.com/support/manual/>.